JOURNAL OF CATALYSIS 146, 292–305 (1994)

In Situ Controlled Promotion of Catalyst Surfaces via NEMCA: The Effect of Na on the Pt-Catalyzed CO Oxidation

I. V. Yentekakis,* G. Moggridge,† C. G. Vayenas,* and R. M. Lambert†

*Institute of Chemical Engineering and High Temperature Chemical Processes, Department of Chemical Engineering, University of Patras, Patras, GR-26500, Greece; and †Department of Chemistry, University of Cambridge, Lensfield Road, Cambridge CB2 1EW, England

Received July 9, 1993; revised October 22, 1993

It was found that the catalytic activity of Pt for CO oxidation can be markedly and reversibly affected by depositing polycrystalline Pt films on β''-Al_2O_3, a Na^+ conductor, and applying external potentials to supply or remove Na to or from the Pt catalyst surface. The change in the rate of CO oxidation is typically 10^3–10^5 times larger than the rate of supply or removal of Na. The use of the β''-Al_2O_3 solid electrolyte supports permits precise *in situ* control of the Na coverage on the Pt surface. Sodium coverages of 0.02 cause up to 600% steady-state increase in the rate of CO oxidation under CO-rich conditions. The promoting effect is due to enhanced oxygen chemisorption on the Pt surface. Higher (>0.06) Na coverages poison the rate severely and reversibly due to the formation of a CO–Na–Pt surface complex. Rate oscillations can be reversibly induced or stopped and their frequency can be controlled by controlling the catalyst potential V_{WR} and average work function $e\Phi$.

INTRODUCTION

The effect of non-Faradaic electrochemical modification of catalytic activity (NEMCA) (1–21) or electrochemical promotion in catalysis (22) has been described for some 20 catalytic reactions on Pt, Pd, Rh, Au, and Ag surfaces (1–21). Work prior to 1992 has been reviewed in Ref. (2). In brief, it has been found that the catalytic (1–21) and chemisorptive (15) properties of polycrystalline metal films interfaced with solid electrolytes, such as yttria-stabilized-zirconia (YSZ), an O^{2-} conductor, or β''-Al_2O_3, a Na^+ conductor, can be affected dramatically and reversibly by electrically polarizing the metal–solid electrolyte interface in cells of the type

gaseous reactants, metal catalyst|solid electrolyte|
counter electrode, air

and thus supplying or removing ions to or from the catalyst surface.

In the case of YSZ solid electrolyte which has been used in most previous studies (1–9, 14–21), the steady-state increase in catalytic rate can be up to 70 times higher than the regular (open-circuit) catalytic rate and up to 3×10^5 times higher than the steady-state rate of O^{2-} supply (2, 5). Pronounced rate modification has been also observed when using β''-Al_2O_3 as the solid electrolyte in the case of C_2H_4 oxidation on Pt (2, 10).

It has been shown both experimentally by means of a Kelvin probe (1, 11) and theoretically (2, 5, 6, 13) that when the catalyst potential V_{WR}, with respect to a reference electrode, changes by ΔV_{WR}, the work function of the catalyst surface $e\Phi$ changes by

$$\Delta(e\Phi) = e\Delta V_{WR}. \quad [1]$$

It has been proposed (1, 2, 4) that this work function change results from an electrochemically controlled spillover of ions from (or to) the solid electrolyte to (or from) the catalyst surface. These spillover ions, together with their compensating charge in the metal spread over the catalyst surface, acting as promoters and establishing an effective electrochemical double layer on the catalyst surface thus altering the catalyst surface work function $e\Phi$ and its chemisorptive and catalytic properties. Recent *in situ* XPS investigation of Ag (23, 24) and Pt (25) catalyst films interfaced with YSZ has confirmed that this is indeed the case (25). The spillover oxide ion, with an O 1*s* binding energy of 528.8 eV (25) is significantly less reactive with H_2 and CO than normally chemisorbed oxygen (O 1*s* binding energy at 530.2 eV) and acts as a catalyst promoter (25). One common conclusion, emerging from all previous studies (1–19), is that over wide ranges of catalyst surface work function $e\Phi$, catalytic rates depend exponentially on $e\Phi$ according to

$$\ln(r/r_0) = \alpha(e\Phi - e\Phi^*)/k_bT, \quad [2]$$

where r_0 is the regular (open-circuit) catalytic rate and α and Φ^* are reaction- and catalyst-specific constants. The value of α is usually between -1 and 1 and, depending

0021-9517/94 $6.00

on its sign, catalytic reactions are termed electrophobic ($\alpha > 0$) or electrophilic ($\alpha < 0$).

The oxidation of CO on Pt is one of the most thoroughly studied catalytic systems (26–31) both because of its importance in automotive exhaust catalysis (31) and because of its well-known oscillatory behaviour (26, 27, 30). Isotopically labelled ^{13}CO has been used to show that the mechanism is of the Langmuir–Hinshelwood type (32). Despite the rich literature on the effect of alkali promoters on CO chemisorption on transition metal surfaces (33–38), there have been no studies on the role of alkali promoters during CO oxidation.

The CO oxidation on Pt was one of the first reactions found to exhibit NEMCA utilizing YSZ as the solid electrolyte (3). During this study it was found that rate oscillations could be induced or stopped at will and their frequency could be controlled by controlling the catalyst potential. Also this study showed a very pronounced (600%) rate increase at very low potential and $e\Phi$ values.

The use of β''-Al_2O_3 to reversibly dose Na on Pt catalyst surfaces and induce NEMCA was first demonstrated for the case of C_2H_4 oxidation on Pt/β''-Al_2O_3 (10). It was found that the rate of CO_2 production could be varied by a factor of 3 and that the Na toxicity was near 50. Furthermore it was shown that the initial dipole moment of Na on polycrystalline Pt is very near the value measured for Na/Pt(111) under UHV conditions (33, 34). In the present work we study the promotional and poisoning effect of Na on the Pt-catalyzed CO oxidation by using β''-Al_2O_3 interfaced with Pt catalyst as the reversible Na donor.

EXPERIMENTAL

The apparatus, utilizing on-line gas chromatography, mass spectrometry (Balzers QMG 311), and IR spectroscopy (Anarad AR-500 CO_2 Analyzer) for continuous analysis of reactants and products has been described in detail elsewhere (2, 3, 30).

The reactor used was of the "single-pellet" type (Fig. 1), i.e. the β''-Al_2O_3 disc was suspended in a quartz well-mixed reactor with the three electrodes, i.e., catalyst, counter and reference, all exposed to the reacting gas mixtures. The relative merits of this "single-pellet" configuration vs the "fuel cell-type" configuration used in most previous NEMCA studies, where the counter and reference electrodes are exposed to air (1–16), have been discussed elsewhere (2, 17, 18). The quartz reactor volume was 25 cm^3.

The Pt catalyst film was deposited on one side of the β''-Al_2O_3 disk (Ceramatec) as described previously, i.e., by using a thin coating of Engelhard Pt A1121 paste followed by calcining in air first at 400°C for 2 h, then at 800°C for 30 min. Three Pt/β''-Al_2O_3 catalyst films (labeled

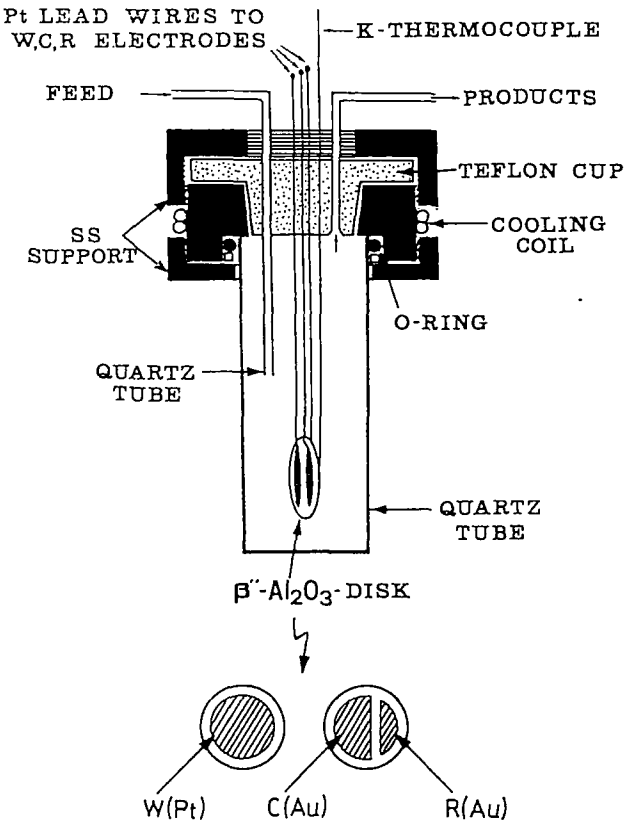

FIG. 1. Single pellet catalytic reactor and electrodes configuration.

C1, C2, and C3) were used in the course of the experiments and all of them showed similar behaviour. Their true surface areas, determined by surface titration as described in detail elsewhere (2, 30) were 248, 98, and 177 cm^2, respectively (Table 1). Catalyst C2 was sintered at 850°C for 30 min (instead of 800°C) and exhibited consistently an offset potential value V_{WR} which was 0.3 V more positive than the others. This offset V_{WR} value remained constant both under open-circuit and closed-circuit operation and must be due to Na contamination of the reference Au electrode due to thermal diffusion of Na during catalyst calcination at 850°C. When this offset potential value is taken into account all three catalysts C1, C2, and C3

TABLE 1

Code	Catalyst	Reactive oxygen uptake of catalyst-electrode (N_0/g-at O)	True catalyst surface area (A/cm^2)
C1	Pt/β''-Al_2O_3	6.3×10^{-7}	248
C2	Pt/β''-Al_2O_3	2.5×10^{-7}	98
C3	Pt/β''-Al_2O_3	4.5×10^{-7}	177
C4	Pt/YSZ	3.7×10^{-7}	146

exhibit exactly the same rate behaviour vs V_{WR}. Thus in figures related to catalyst C2 we show both the raw V_{WR} values (denoted by V'_{WR}) and the corrected V_{WR} values obtained by subtracting the offset potential value. The fourth catalyst (C4) of Table 1 was a similarly prepared Pt catalyst film deposited on YSZ. This was done in order to compare turnover frequencies under open circuit conditions of Pt/β''-Al_2O_3 and Pt/YSZ as described below.

The Au counter and reference electrodes were deposited on the other side of the β''-Al_2O_3 disk (Fig. 1) using Demetron M8032 Au paste followed by calcination at 800°C. Since Au supported on several oxides (Fe_2O_3, Co_3O_4, and TiO_2) has been recently reported (39) to be fairly active for CO oxidation even at room temperature, a series of blank experiment was conducted without the Pt catalyst film to assess the relative importance of the Au-catalyzed reaction. It was found that the rate due to Au accounts for less than 5% of the rate in presence of Pt and thus, its catalytic effect, can be to a good approximation, neglected. Furthermore, in a series of experiments where the Pt catalyst was used as a reference electrode and currents and potentials were applied between the Au counter and Au reference electrodes, no change in the rate was observed. Thus all the current- and potential-induced changes in catalytic activity described below can be safely attributed to Pt only. Reactants were L'Air Liquide certified standards of 10% CO in He and 20% O_2 in He. They could be further diluted in ultrapure He (99.999%).

Since catalyst preparation inevitably results in some contamination of the Pt catalyst surface due to thermal migration of Na from the β''-Al_2O_3 structure during catalyst sintering at 800°C, the following procedure was followed in order to eliminate as much as possible this contamination and define a "clean" and, certainly, reproducible state of the Pt catalyst surface: A potential difference $V_{WR} = +400$ mV was applied between the catalyst and reference electrode at $T = 400$°C until the current ($I > 0$) between the catalyst and counter electrode vanished. This current corresponds to the reaction:

$$Na(Pt) \leftrightharpoons Na^+(\beta''\text{-}Al_2O_3) + e^- \qquad [3]$$

In this way the initially contaminated Pt surface can be cleaned (10). As shown below, similarly to the case of C_2H_4 oxidation on Pt/β''-Al_2O_3 (10), there is a one-to-one correspondence between V_{WR} and catalytic rate, therefore the potentiostatic mode of operation is much more advantageous when using β''-Al_2O_3 solid electrolytes. The galvanostatic (constant current) mode of operation is useful only for studying transients and extracting initial dipole moment values, as described below. With the exception of these transient experiments, all other results reported here were obtained potentiostatically, i.e., by setting V_{WR} at constant values.

A separate set of experiments, utilizing a Kelvin probe (Besocke/Delta-Phi-Electronik, probe "S") to measure *in situ* the work function $e\Phi$ of the gas-exposed surface of Pt electrodes interfaced with β''-Al_2O_3, as well as with YSZ, and exposed to $CO/O_2/He$ as well as $NH_3/O_2/He$ atmospheric pressure mixtures (1, 2, 11) has confirmed the theoretical proposition (2, 5) that the change in the potential V_{WR} of solid electrolyte cells with metal electrodes is directly related, both under open-circuit and closed-circuit conditions (1, 2, 11), to the change in work function $e\Phi$ of the gas-exposed catalyst electrode surface via

$$\Delta(e\Phi) = e\Delta V_{WR}; \qquad [1]$$

i.e., solid electrolyte cells with metal electrodes are both work function probes and work function controllers (when an external voltage is applied) for their gas-exposed electrode surfaces.

In order to simplify the catalytic reactor design (Fig. 1) the work function $e\Phi$ was not monitored in situ via the Kelvin probe in the present kinetic investigation and Eq. [1], confirmed within 5% under practically identical conditions (1, 2, 11) was used to compute $\Delta(e\Phi)$ and present it as a second absisca together with V_{WR}.

It is worth noting that eV_{WR} equals the difference in work function $e\Phi$ of the catalyst and reference electrodes (1, 2). Thus, although reaction [3] is the dominant potential-setting reaction at all three electrodes (working, counter, and reference, Ref. 10), an equivalent fundamental non-Nerstian physical meaning of eV_{WR} is that it reflects the difference in work function of the gas-exposed surfaces of the catalyst and reference electrodes (1, 2).

RESULTS

General features. In order to facilitate the detailed presentation and discussion of results we first show (Figs. 2 and 3) the main general trends observed upon varying catalyst potential V_{WR}.

The data shown in Fig. 2 exemplify the two typical types of behaviour obtained upon varying catalyst potential V_{WR}, which as discussed above is directly related (1, 2) to the catalyst work function $e\Phi$ via Eq. [1].

As previously noted, V_{WR} values above 0.4 V correspond to a Na-free Pt catalyst surface. The first type of behaviour, labelled "S"-type behaviour in Fig. 2, is obtained when the rate on the Na-free Pt surface is positive order in CO (see also Fig. 3): Upon decreasing V_{WR} and thus supplying Na to the surface, thereby decreasing $e\Phi$, the rate is practically unaffected and then at $V_{WR} = -0.3$ V decreases abruptly to a much lower value. This

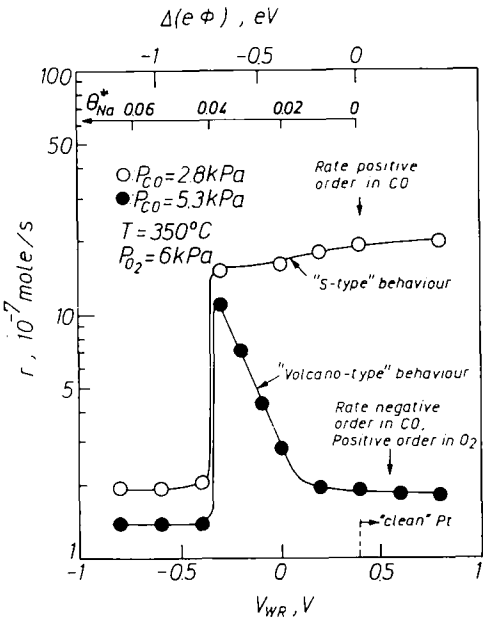

FIG. 2. Effect of catalyst potential V_{WR}, corresponding work function change $\Delta(e\Phi)$, and approximate linearized Na coverage θ^*_{Na} on the rate of CO oxidation. Conditions: T = 350°C, P_{O_2} = 6 kPa, P_{CO} = 5.3 kPa (filled symbols), P_{CO} = 2.8 kPa (open symbols); catalyst C1.

abrupt transition takes place at a total Na coverage θ_{Na} value near 0.05, as is subsequently shown in this paper on the basis of coulometric measurements during galvanostatic transients.

The second type of behaviour, labeled "volcano-type" behaviour in Fig. 2 is obtained when the rate on the Na-free Pt surface ($V_{WR} > 0.4$ V) is negative order in CO and positive order in O_2 (see also Fig. 3). Upon decreasing V_{WR} below 0.4 V the rate increases exponentially with $-V_{WR}$ and θ_{Na}, i.e., Na acts as a *promoter* and enhances the catalytic rate r by ~500%. (Figs. 2 and 3). Then at $V_{WR} = -0.3$ V this exponential rate increase comes to an abrupt end and r drops precipitously by a factor of 8 stabilizing to a new low value. As will be subsequently shown this abrupt rate decrease corresponds in this case to $\theta_{Na} \approx 0.03$, i.e., the exact ΔV_{WR} vs θ_{Na} relationship depends on the surface coverages of CO and O and thus on gaseous composition.

Despite this complication we have chosen for a more simplified presentation to show additionally in Figs. 2, 3, and subsequent figures an approximate linear inserted Na coverage scale labelled hereafter θ^*_{Na} to distinguish from the precisely measured coulometrically Na coverage θ_{Na} also shown in some of the figures. This linear approximate θ^*_{Na} scale is constructed via the Helmholz Equation,

$$\theta^*_{Na} = -\varepsilon_0 \Delta(e\Phi)/(eP_0 N_{Pt}), \quad [4]$$

where $\varepsilon_0 = 8.85 \times 10^{-12}$ C²/(J · m), $e = 1.6 \times 10^{-19}$ C/atom, P_0 is the dipole moment of Na on Pt, and $N_{Pt} = 1.53 \times 10^{19}$ atom/m² is the surface Pt concentration on the Pt(111) plane. In constructing the θ^*_{Na} scale, a P_0 value of 1.20×10^{-29} C m, or 3.6 D was used. As shown below this value provides a reasonably good fit to the $\Delta e\Phi$ vs θ_{Na} data and is 40% lower than the initial dipole moment of Na on Pt(111) (33, 34) and on similar polycrystalline Pt films (2, 10, 11). This difference is due to the strong attractive interaction of CO and Na as discussed below, where it is shown that θ^*_{Na} and θ_{Na} can differ by up to a factor of two.

It is noteworthy in Fig. 2, that in both cases, i.e., "S-type" or "volcano-type" behaviour, the transition to a low rate value takes place at practically the same V_{WR} value. As shown below this is due to formation of a CO–Na–Pt complex on the catalyst surface, similar to the CO–K–Pt surface complex detected by TDS on Pt(100) at temperatures below 400°C (40).

The above features can be seen more clearly in the three-dimensional Figs. 3a, 3b, and 3c obtained by fitting a large number of data (~100) at T = 350°C and P_{O_2} = 6 kPa to a polynomial expression. Thus on the clean Pt surface ($V_{WR} > 0.4$ V) one sees the classical Langmuir–Hinshelwood type rate dependence on P_{CO}. Then as V_{WR} is decreased the rate is very significantly enhanced for high P_{CO} values and is only very weakly decreased for low P_{CO} values where the rate is positive order in CO. In both cases an abrupt rate decrease takes place at $V_{WR} = -300$ mV due to the CO–Na–Pt complex formation. Consequently, upon varying V_{WR}, "S-type" behaviour is obtained for low P_{CO} and "volcano-type"-behaviour is obtained for high P_{CO} values.

Transient effect of applied constant current. Figures 4a and 4b show typical galvanostatic transients, i.e., they depict the effect of applying a constant negative current (Na supply *to* the catalyst) on catalyst potential V_{WR} and rate r of CO oxidation.

Figure 4a corresponds to "volcano-type" behaviour, i.e., P_{O_2}, P_{CO}, and T were chosen such that the rate on the Na-free Pt surface is negative-order in CO. What is remarkable is that this "volcano-type" behaviour is also manifested in the transient mode (Fig. 4a, rate response). We first concentrate on the solid V_{WR} and r lines which correspond to an initial potentiostatically imposed V_{WR} value of 0.4 V ($t < -1$ min). The potentiostat is then disconnected ($I = 0$, $t = -1$ min) and V_{WR} relaxes to ~0 V, i.e., to the value imposed by the gaseous composition and corresponding surface coverages of O and CO. There is a small (~30%) corresponding increase in r. Then at $t = 0$ the galvanostat is used to impose a constant current $I = -20$ μA; Na^+ is now pumped to the catalyst surface at a rate $I/F = 2.07 \times 10^{-10}$ g-atom Na/s. The correspond-

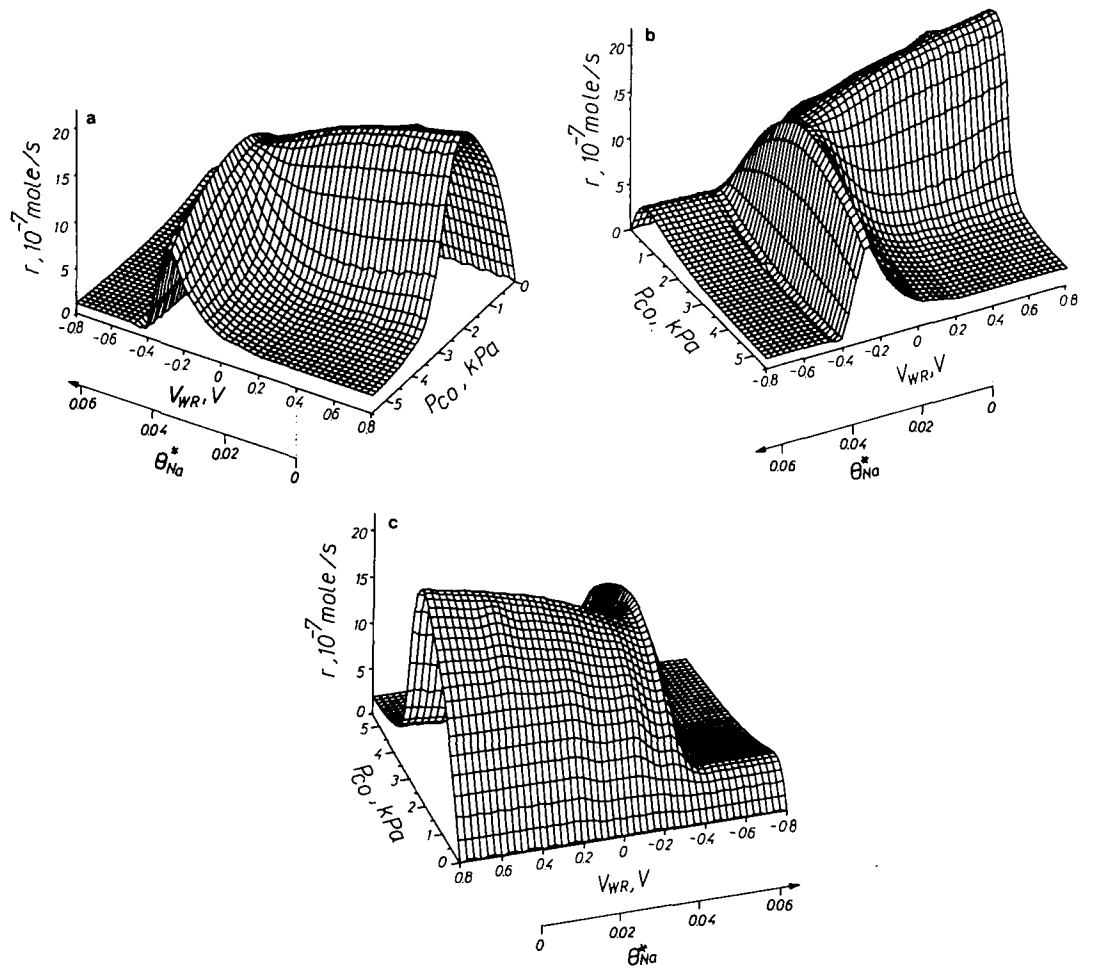

FIG. 3. (a, b, c) Three-dimensional presentation of the effect of P_{CO} and catalyst potential V_{WR} on the rate of CO oxidation. Conditions: T = 350°C, P_{O_2} = 6 kPa; catalyst C1.

ing Na coverage on the Pt surface θ_{Na} can be computed from Faraday's Law, i.e.,

$$\frac{d\theta_{Na}}{dt} = \frac{I}{F \cdot N_0}, \qquad [5]$$

where N_0 is the number of available Pt sites (6.3×10^{-7} g-atom Pt) independently measured via surface titration. Thus the inserted precise θ_{Na} abscissa in Fig. 4a may be constructed.

Increasing θ_{Na} up to 0.02 causes a linear decrease in V_{WR} and $e\Phi$ and a concomitant 230% *increase* in catalytic rate. When θ_{Na} reaches 0.02, V_{WR} and $e\Phi$ remain constant ($V_{WR} = -0.3$ V) for 2 min ($0.02 < \theta_{Na} < 0.06$) while r decreases sharply and reaches values below the initial value. When θ_{Na} exceeds 0.06, V_{WR} and $e\Phi$ start to decrease sharply while r remains practically constant.

Setting $I = 0$ gradually restores V_{WR} to -0.3 V while r remains unaffected. Restoration of the initial r value requires potentiostatic setting of V_{WR} to $+0.4$ V. It is noteworthy that the r vs t or, equivalently r vs V_{WR} behaviour depicted in Fig. 4a is qualitatively similar to the steady-state r vs V_{WR} behaviour shown in Figs. 2 and 3. Thus the catalyst surface readjusts fairly fast to the imposed θ_{Na} values, although in general the induced rate changes are smaller, as no true steady state is attained during the transients.

The dashed and dotted line transients depicted in Fig. 4a where obtained with the same gaseous composition but with initial V_{WR} values of 0 and -0.3 V, respectively. It is noteworthy that the three transients are very similar to each other as they exhibit the same qualitative features.

The galvanostatic transient shown in Fig. 4b corresponds to "S-type" behaviour, i.e., the rate r_0 on the Na-free Pt surface is first-order in CO. Initially ($t < -0.5$ min) V_{WR} is maintained at $+0.4$ V by means of the potenti-

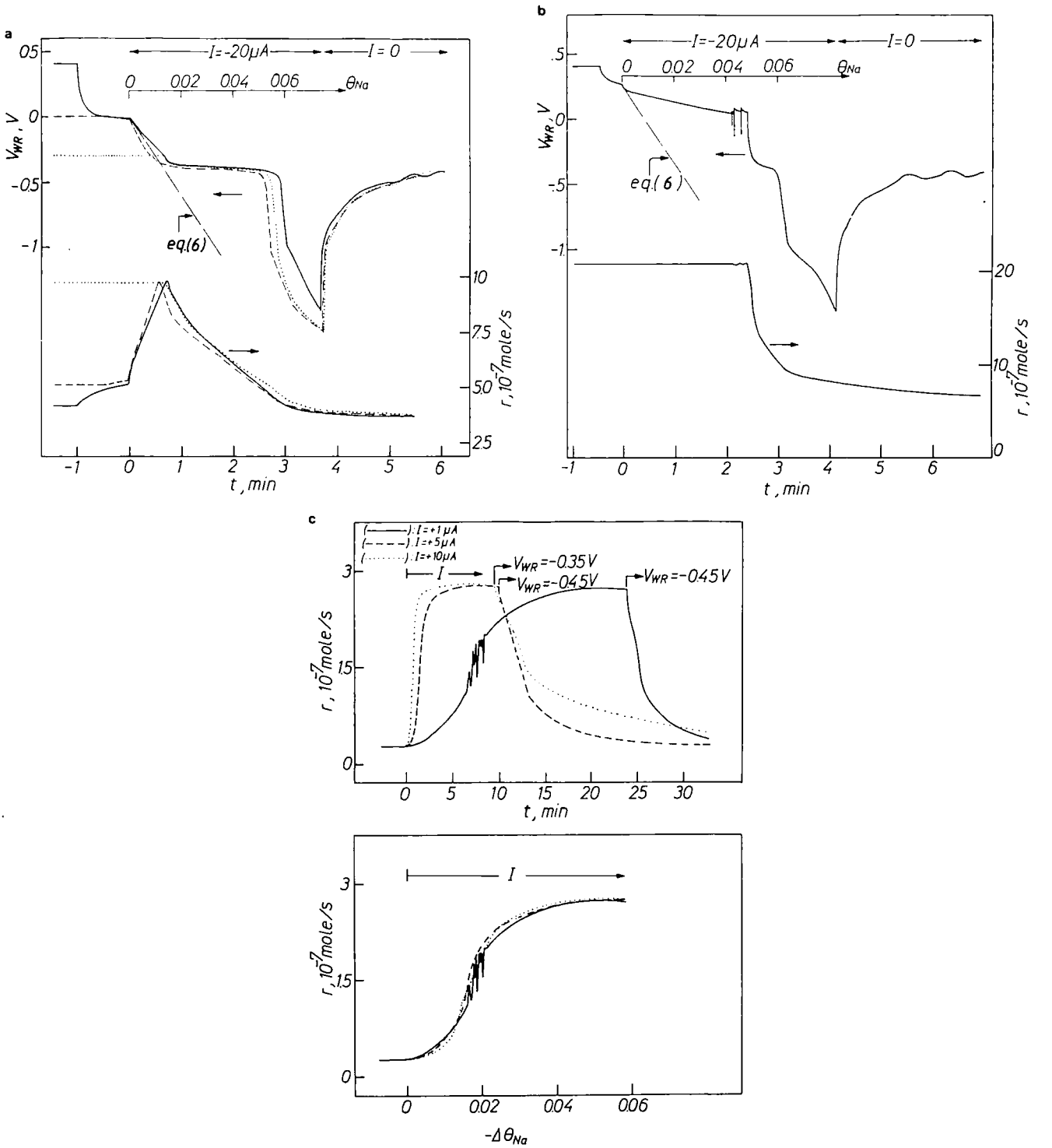

FIG. 4. Rate and catalyst potential response to application of negative currents (a, b), for the case of "volcano-type" behaviour (a), and "S-type" behaviour (b) of the reaction rate. Rate response to application of positive currents (c); see text for discussion. Conditions: (a) P_{CO} = 2 kPa, P_{O_2} = 2 kPa, T = 350°C; catalyst C1. (b) P_{CO} = 2 kPa, P_{O_2} = 4 kPa, T = 350°C; catalyst C1. (c) P_{CO} = 0.73 kPa, P_{O_2} = 0.86 kPa, T = 402°C, catalyst C2.

ostat. At $t = -0.5$ min the potentiostat is disconnected ($I = 0$) and V_{WR} relaxes to +0.3 V without any measurable r change. Then at $t = 0$, a current $I = -20$ μA is imposed and Na^+ is supplied to the catalyst at a rate $I/F = 2.07 = 10^{-10}$ g-atom Na/s. There is a gradual decrease in V_{WR} and $e\Phi$ while r remains unaffected. When θ_{Na} reaches 0.05 the rate decreases sharply by more than 50% with a concomitant sharp decrease in V_{WR} and $e\Phi$.

The slopes in Figs. 4a and 4b correspond to the differentiated Helmholz equation derived previously (10),

$$\frac{edV_{WR}}{dt} = \frac{d(e\Phi)}{dt} = \frac{P_0 I}{\varepsilon_0 \cdot A}, \qquad [6]$$

where $P_0 = 1.75 \times 10^{-29}$ C m (5.3 Debye) is the literature initial dipole moment of Na on Pt (33, 34), $\varepsilon_0 = 8.85 \times 10^{-12}$ C^2/J m, and A is the Pt film surface area (2.48×10^{-2} m^2, computed from $N_0 = 6.3 \times 10^{-7}$ g-atom Pt and the Pt(111) atom density, $d = 1.53 \times 10^{19}$ atoms/m^2).

It is worth noting that Eq. [6] provides a nice fit to the initial slopes of the V_{WR} vs t plots (Figs. 4a and 4b). The subsequent leveling of V_{WR} in Fig. 4a is indicative of the formation of the CO–Na–Pt surface complex. Once the complex formation is complete, V_{WR} and $e\Phi$ decrease again abruptly. In Fig. 4b, obtained on a Pt surface predominantly covered with O, significant deviations from Eq. [6] start from very low Na coverages, indicating a substantial decrease in the dipole moment of Na from the value of 5.3 Debye obtained on a clean Pt surface (33, 34). This indicates a strong attractive interaction between adsorbed Na and O leading to the formation of a Na–O–Pt complex. The formation of stable ultra thin films of alkali oxides, peroxides and superoxides on clean metal surfaces is well documented (41).

Figure 4c shows the transient effect of positive current application, i.e., of Na removal from the catalyst under conditions of "S-shaped" type behaviour. Electrochemical Na removal from the initially Na-contaminated catalyst results in 1000% increases in catalytic rate. Potentiostatic restoration of the initial V_{WR} value (-0.35 or -0.45 V as shown in the figure), restores the initial rate value. It is noteworthy that different currents cause the same rate increase, albeit over different time periods. However, when replotting the results in terms of $\Delta\theta_{Na}$ computed from

$$\Delta\theta_{Na} = \frac{-It}{FN_0}, \qquad [7]$$

a single curve results both for r and for V_{WR}, demonstrating the one-to-one correspondence between θ_{Na}, V_{WR}, and r (see bottom diagram in Fig. 4c).

Effect of P_{CO}. Figure 5a shows the effect of P_{CO} on reaction rate at various fixed values of V_{WR}. Because of the relatively high T and P_{O_2} values, "S-type" behaviour is favoured, upon varying V_{WR}.

For $V_{WR} = +1$ V ($V_{WR} = 0.7$ V) the Pt surface is Na-free and, as shown in the figure, the kinetics (turnover

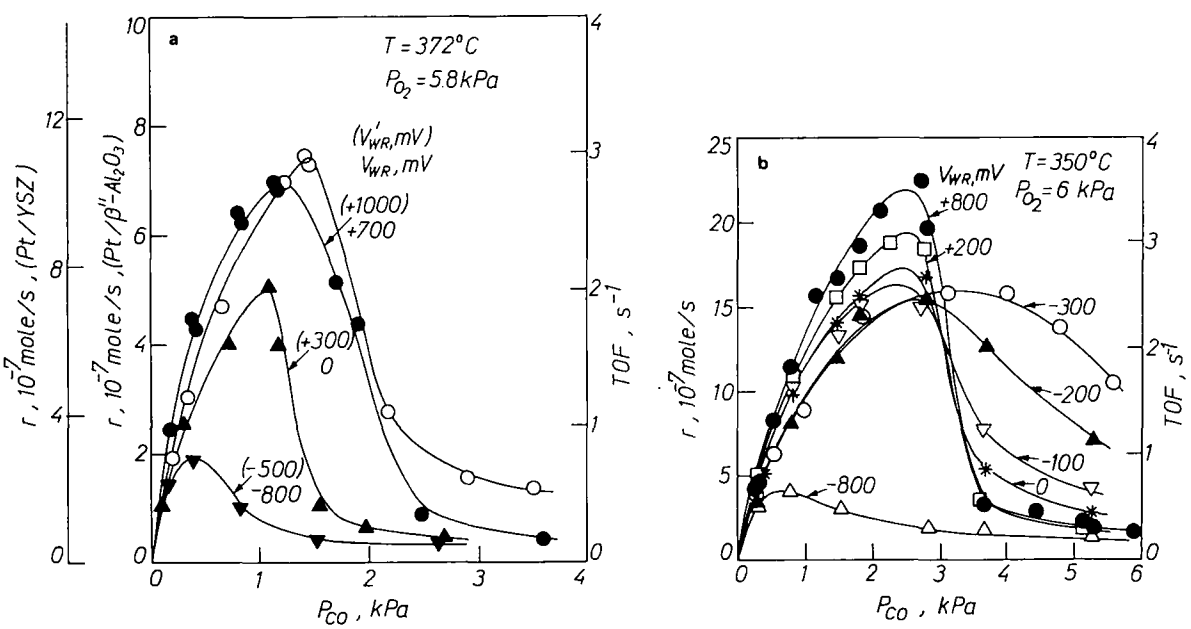

FIG. 5. Effect of partial pressure of CO (P_{CO}) on reaction rate at varying catalyst potential V_{WR} (V'_{WR} is the uncorrected for the offset voltage V_{WR} value of catalyst C2). Conditions: (a) $T = 372$°C, $P_{O_2} = 5.8$ kPa, (("S-type" behaviour) catalyst C2; open symbols correspond to Pt/YSZ catalyst C4. (b) $T = 350$°C, $P_{O_2} = 6$ kPa, ("volcano-type" behaviour) catalyst C1.

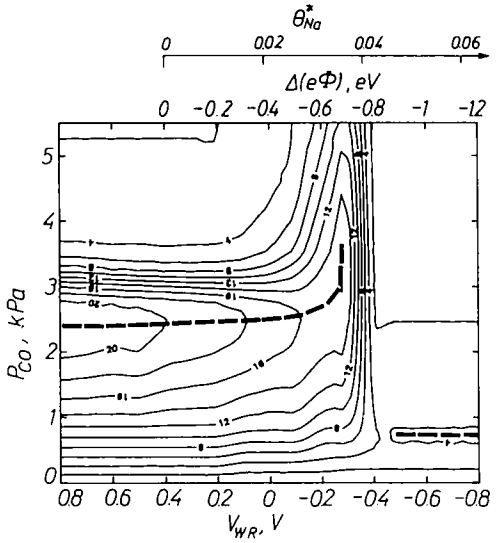

FIG. 6. Topographic view of the effect of P_{CO} and V_{WR} on the rate of CO oxidation. The variation of P^*_{CO} vs P_{CO} and V_{WR} is noted by the broken line. Conditions as in Fig. 3.

frequencies) are in good qualitative agreement with those measured on similar polycrystalline Pt films deposited on YSZ.

Decreasing V_{WR} below the value corresponding to CO–Na–Pt complex formation causes a decrease in the rate and a concomitant decrease of P^*_{CO} (hereafter denoting the P_{CO} value which maximizes r). This is also depicted in Fig. 6 which shows the variation in P^*_{CO} with V_{WR}.

Figure 5b depicts a situation where "volcano-type" and "S-type" behaviour is obtained for high and low P_{CO} values, respectively. It is noteworthy that in the volcano region P^*_{CO} is significantly increased in comparison with the Na-free Pt indicating a significantly greater strengthening of the Pt–O relative to the Pt–CO bond. This is also shown in Fig. 6.

The sudden transition from −300 to −800 mV is due to formation of the CO–Na–Pt surface complex which we recently demonstrated by TDS to form on Pt(111) (Ref. (42); compare also with Figs. 2 and 3). At this point P^*_{CO} also decreases abruptly, indicating a relative strengthening in the Pt–CO vs the Pt–O bond.

Effect of P_{O_2}. Figure 7 shows the effect of P_{O_2} and V_{WR} on r at constant P_{CO}. It must be noted first that for low P_{O_2} values the behaviour with respect to V_{WR} is volcano-type, i.e., r is maximized at $V_{WR} \approx -0.3$ V. For intermediate P_{O_2} values the behaviour with respect to V_{WR} is "S-type." The main feature of Fig. 7 is the observed sharp rate increase with increasing P_{O_2} at $P_{O_2} \approx 2.5$ kPa. It is noteworthy that this sharp rate increase, which is indicative of a surface phase transition takes place also for $V_{WR} = +0.5$ V, i.e., on the Na-free Pt surface as well. This sharp rate transition is very likely due to the breaking of large chemisorbed CO islands by intrusion of O adatoms which weakens substantially the strength of the Pt–CO bond and leads to a remarkable decrease in the activation energy of the reaction as shown by a recent study of the kinetics of CO oxidation on clean Pt(111) (43).

As also shown on Fig. 7 for low V_{WR} values (−800 mV), where formation of the CO–Na–Pt surface complex (42) takes place, there is significant counterclockwise hysteresis when starting with the catalyst preexposed overnight in CO. In this case as P_{O_2} is increased there is a gradual destruction of the CO–Na–Pt surface complex which is complete at $P_{O_2} = 10$ kPa. Upon subsequently decreasing P_{O_2} the rate follows a different path until the point is reached where the surface gets predominantly covered by CO, which causes a sharp rate decrease as observed for the other V_{WR} values as well. The remaining hysteresis for $V_{WR} = -800$ mV and very low values (<2 kPa) P_{O_2} is likely to indicate a different stoichiometry of the CO–Na–Pt complex originating from a different micromorphology of the CO islands on the surface resulting from the different gaseous pretreatment.

Effect of V_{WR}, *and Na coverage.* Figures 8a, 8b, 9, and 10 show the effect of V_{WR}, work function $e\Phi$ and approximate Na coverage θ^*_{Na} on the rate of CO oxidation, while holding two of the parameters P_{CO}, P_{O_2}, and T constant and varying the third. In the case of Fig. 8a, the Na coverage θ_{Na} has also been measured precisely, via coulometry, as shown in the top part of the figure and

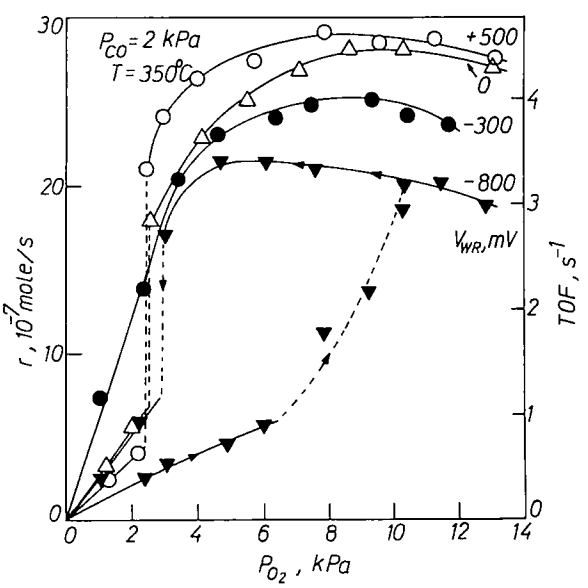

FIG. 7. Effect of P_{O_2} on the rate of CO oxidation at varying catalyst potential V_{WR}. Conditions: $P_{CO} = 2$ kPa, $T = 350$°C; catalyst C1.

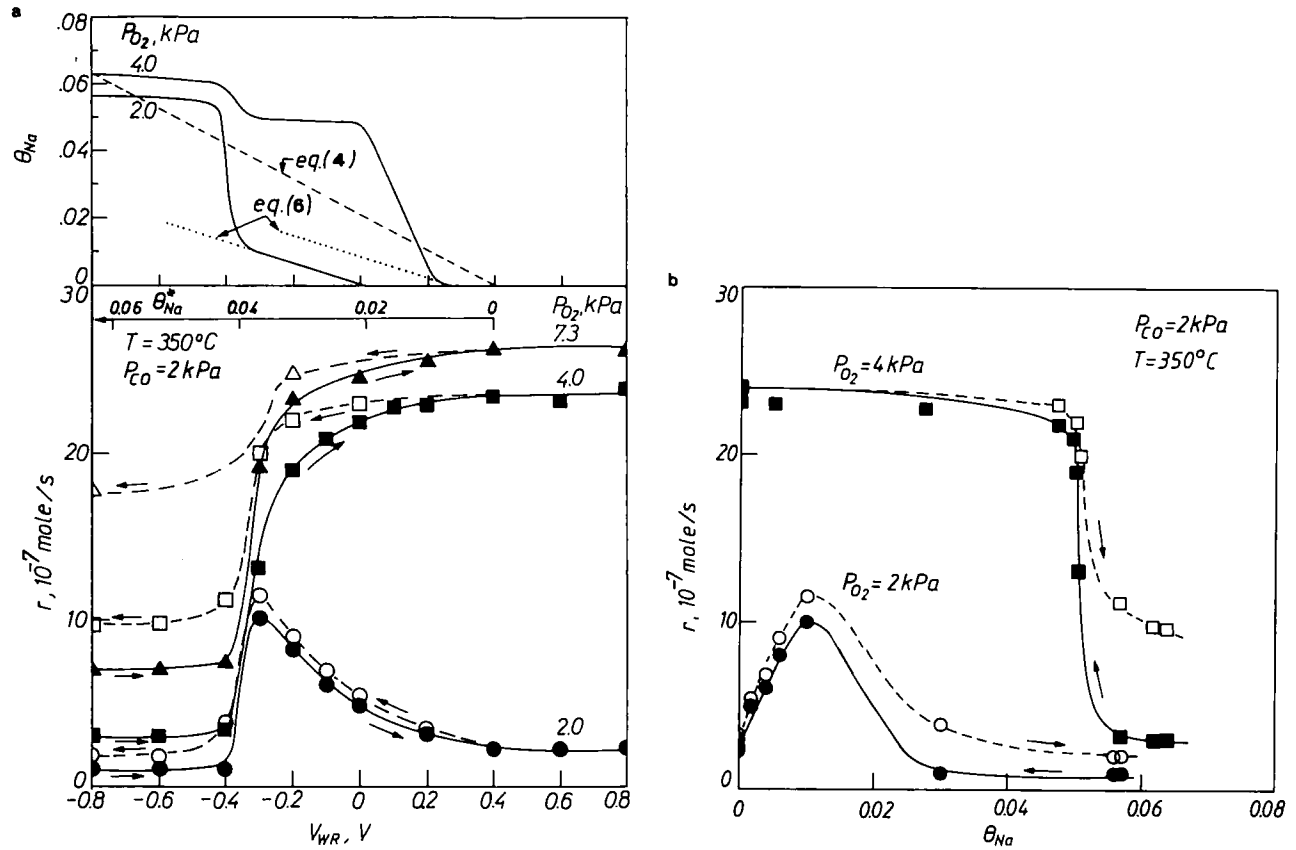

FIG. 8. (a) Effect of V_{WR} on the rate of CO oxidation at varying P_{O_2}. Other conditions: P_{CO} = 2 kPa, T = 350°C. The top part of the figure shows the corresponding variation of θ_{Na} with V_{WR}; catalyst C1. (b) Effect of Na coverage θ_{Na} on the rate of CO oxidation. Conditions as in (a).

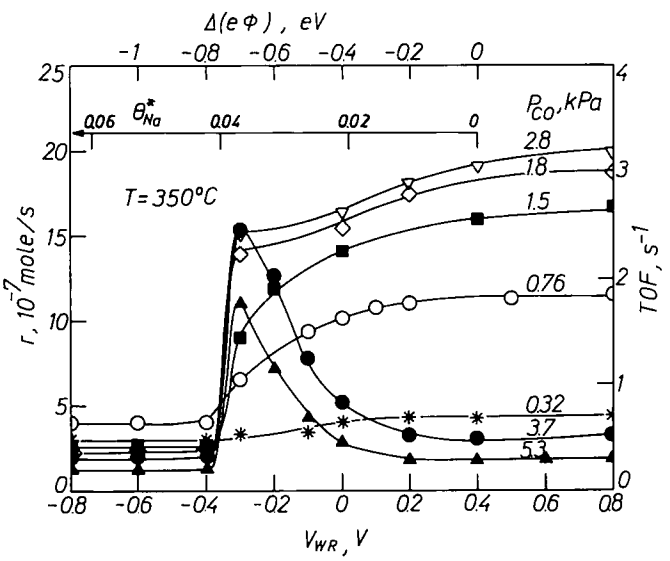

FIG. 9. Effect of V_{WR} on the rate of CO oxidation at varying P_{CO}. Other conditions: P_{O_2} = 6 kPa, T = 350°C; catalyst C1.

thus Fig. 8b was obtained which depicts directly the effect of θ_{Na} on the rate at constant P_{CO}, P_{O_2}, and T.

Thus Fig. 8a depicts the effect of V_{WR} and P_{O_2} while holding P_{CO} and T constant. High P_{O_2} values favour S-type behaviour and low P_{O_2} values favour volcano-type behaviour. The figure also shows the hysteresis obtained when starting with the catalyst maintained overnight in CO at V_{WR} = −800 mV. The origin of this hysteresis was discussed above in conjunction with the effect of P_{O_2}. In the case of S-type behaviour (P_{O_2} = 4 kPa) the rate decreases abruptly at V_{WR} = −0.3 V due to CO–Na–Pt complex formation. In the case of volcano-type behaviour, Na has a promoting effect on the rate until again the point is reached where the CO–Na–Pt complex forms.

The top part of Fig. 8a shows the corresponding coulometrically determined variation in θ_{Na} with V_{WR} for the cases P_{O_2} = 2.0 and 4.0 kPa. The initial θ_{Na} vs V_{WR} slopes are again in good agreement with Eq. [6]. The subsequent sharp rise in θ_{Na} at V_{WR} = −0.3 V is indicative of the CO–Na–Pt complex formation. This rise is more pro-

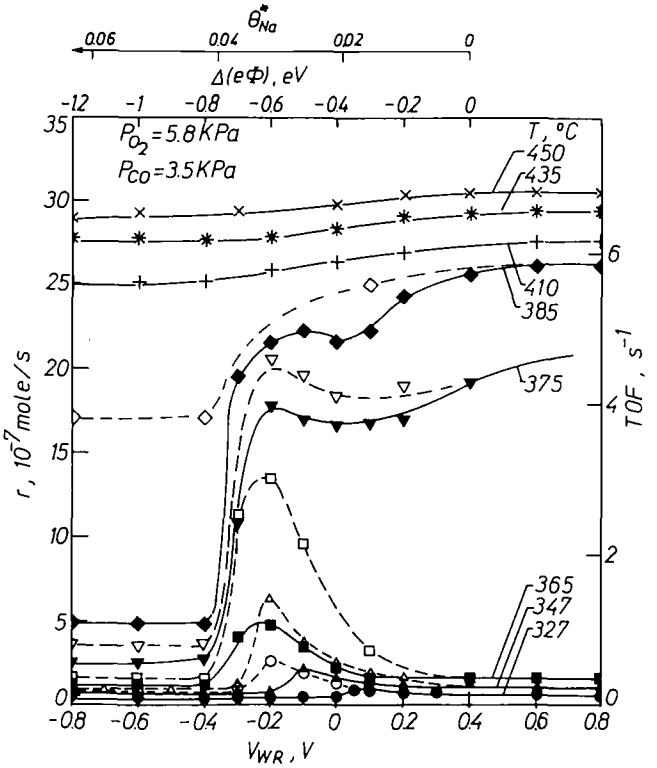

FIG. 10. Effect of V_{WR} on the rate of CO oxidation at varying T. Other conditions: P_{O_2} = 5.8 kPa, P_{CO} = 3.5 kPa; catalyst C3.

nounced in the case P_{O_2} = 2 kPa, as the CO coverage is larger. In the case P_{O_2} = 4 kPa the initial sharp increase in θ_{Na} is indicative of a strong attractive interaction between Na and O as analyzed above. As shown in the figure these strong attractive interactions lead to significant variations in the slope of θ_{Na} vs $\Delta(e\Phi)$, thus in dipole moment P_0 and therefore in pronounced deviations of θ^*_{Na} from θ_{Na}.

Figure 8b is obtained by crossploting the results of Fig. 8a and shows directly the effect of the, precisely measured, Na coverage θ_{Na} on the rate of CO oxidation. As expected, the effect of θ_{Na} is very similar to that of $-V_{WR}$ and $-e\Phi$. Volcano-type behaviour is obtained for CO-rich conditions and S-type behaviour is observed for O_2 rich conditions. In the former case θ_{Na} values of 0.02 cause a 500% increase in the rate, underlining the dramatic promoting effect of Na. In both cases θ_{Na} values of 0.03 and 0.05, respectively, suffice to almost entirely poison the rate.

In Fig. 9, P_{O_2} and T are held constant while P_{CO} and V_{WR} are varied. High (≥2 kPa) P_{CO} values, where the rate is negative order in CO, lead to volcano-type behaviour.

Low P_{CO} values, where the rate is positive order in CO lead to S-shaped-type behaviour. In these cases, although Na promotes O_2 chemisorption, there is no enhancement in the rate as the surface has already a sufficiently high oxygen coverage.

Figure 10 shows the effect of V_{WR} and T on the rate at fixed P_{CO} and P_{O_2}. Temperatures below 375°C lead to volcano-type behaviour, while for 375°C < T < 385°C there is S-type behaviour, followed by a situation where V_{WR} has very little effect on the rate. It is clear that under these latter conditions the CO–Na–Pt complex does not form. Under these conditions the rate is positive order both in CO and O_2 and the activation energy is very low (2–3 kcal/mol). The observed behaviour is in excellent agreement with our UHV TDS investigation of the CO–Na–Pt complex on Pt(111) which showed that the complex decomposes at 360°C under UHV (42). The decomposition temperature observed here is higher (~400°C), consistent with the high CO pressure.

A very important common feature of Figs. 8a, 8b, 9, and 10 which is also manifested in Figs. 2 and 7 is the very abrupt rate transition from a low to a high r value observed for $V_{WR} > 0$ (i.e., for a clean or mildly Na-contaminated Pt surface) upon increasing P_{O_2} and T or upon decreasing P_{CO}. This abrupt rate transition is, of course, the result of the abrupt rate decrease when P_{CO} exceeds P^*_{CO} manifested in Figs. 3 and 5 for $V_{WR} > 0$. This transition reflects the change from a predominantly CO-island covered to a predominantly O-island covered Pt surface and is also accompanied by a very pronounced change in activation energy.

Activation energies. Apparent activation energies E were measured from Arrhenius plots at various fixed values of V_{WR} and the results are shown on Fig. 11. Filled symbols correspond to E values below 360°C and open symbols to E values obtained above 360°C. (The exact T at which this rather abrupt transition from a high to a low E value takes place is shown in the insert figure). The situation depicted in Fig. 11 corresponds to volcano-type behaviour.

For $V_{WR} > 0.4$ V it is E = 28 kcal/mol and E remains practically constant as V_{WR} decreases to 0 V. In the region 0 to −300 mV where the rate increases sharply with decreasing V_{WR} (Fig. 8a), E also increases sharply to a value of 52 kcal/mol. By further decreasing V_{WR} ($V_{WR} < -0.3$ V), which causes a sharp decrease in the rate (Fig. 8a), E further increases to 65 kcal/mol. This interesting behaviour is explained in the Discussion, where on the basis of a simple Langmuir–Hinshelwood–Hougen–Watson (LHHW) model the dashed lines shown on Fig. 11 are obtained.

Induction of oscillatory states. Figure 12a shows rate oscillations obtained near the rate transition under S-shape type conditions. Since V_{WR} was held constant, these rate oscillations were accompanied by small (<5 μA) current oscillations. As shown in the figure the V_{WR} range

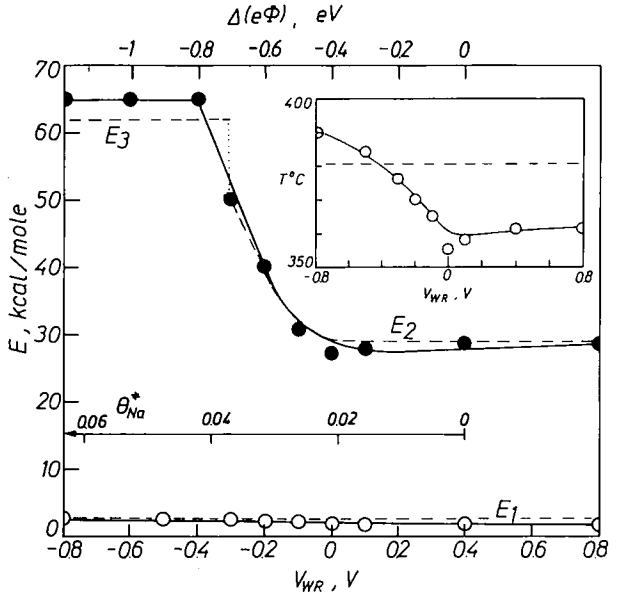

FIG. 11. Effect of catalyst potential V_{WR} on the apparent activation energy, and on the temperature (insert figure) at which the transition occurs from a high (filled symbols) to a low (open symbols) E value. Dashed lines from the model discussed in the text. Conditions: P_{O_2} = 5.8 kPa, P_{CO} = 3.5 kPa; catalyst C3.

over which r oscillates is rather narrow. During each oscillation, increasing r corresponds to $I > 0$, i.e., to Na removal from the catalyst. It is likely that these oscillations are not of the usual type obtained on Pt during CO oxidation (26, 27, 30) but are due to cyclic formation and decomposition of the CO–Na–Pt complex. As shown in the bottom diagram of Fig. 12b the frequency of oscillations increases linearly with V_{WR}.

DISCUSSION

The present results show that β''-Al_2O_3 can be used as an active support to alter the catalytic properties of Pt for CO oxidation in a very pronounced and reversible manner via the NEMCA effect. The β''-Al_2O_3 solid electrolyte acts as a reversible Na^+ donor which permits precise in situ control of the Na coverage on the Pt surface. Sodium is found to have a very pronounced promoting and also poisoning effect on the rate of CO oxidation. The promoting effect dominates when the rate is negative order in CO for low (<0.04) Na coverages and gives up to 600% increases in catalytic rate. Higher (>0.04) Na coverages lead to severe poisoning (up to 90% decrease in the rate) under all conditions.

The enhancement factor or "Faradaic efficiency" (1–19) Λ values obtained in this study are typically of order 10^3–10^5. However, when using a Na^+ donor, such as β''-Al_2O_3, in NEMCA studies, Λ is not a very meaningful quantity, as Na is not a reactant or product and thus in principle "infinitely" large Λ values can be obtained at steady state potentiostatic operation, i.e., if the current were to vanish at steady-state after having caused a steady-state rate increase Δr. In practice this was not found to happen and Λ was always finite ($<10^5$) as it was found that a small parasitic current (~1 μA) always remains at steady-state potentiostatic operation apparently due to the formation of some Na_2O and/or Na_2CO_3 on the catalyst surface, similarly to the case of the NEMCA study of C_2H_4 oxidation on Pt using β''-Al_2O_3 (10).

A more meaningful parameter for expressing the promoting or poisoning effect of Na^+ in NEMCA studies utilizing β''-Al_2O_3, or in promotion studies in general, is the promotion index P_i defined from

$$P_i \equiv \frac{(\Delta r/r_0)}{\Delta\theta_{Na}}, \qquad [8]$$

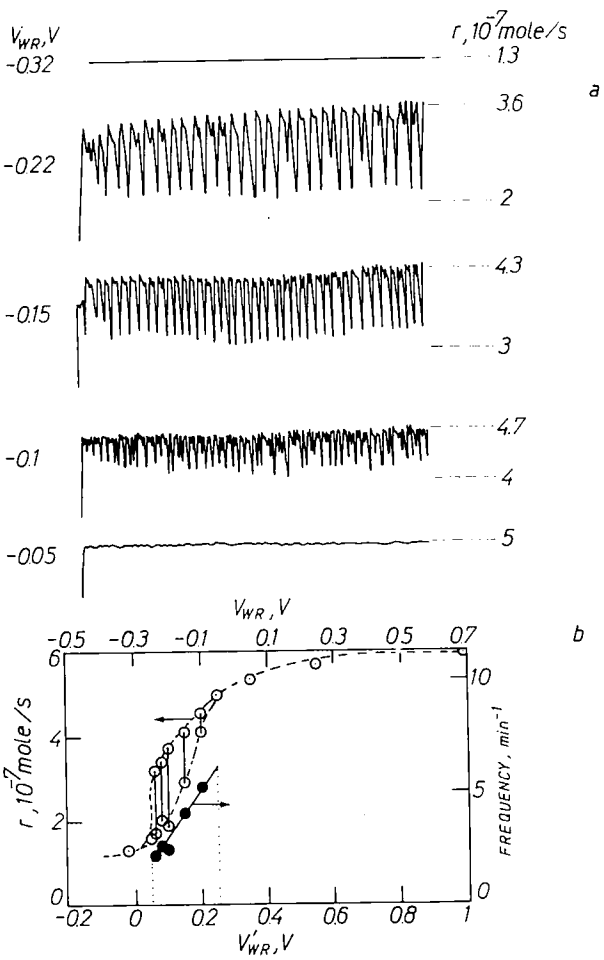

FIG. 12. Effect of catalyst potential V_{WR} on the CO oxidation rate oscillations. Conditions: P_{CO} = 0.95 kPa, P_{O_2} = 9.9 kPa, T = 370°C; catalyst C2.

or, in general,

$$P_i \equiv \frac{(\Delta r/r_0)}{\Delta\theta_P}, \qquad [9]$$

where θ_P is the coverage of the doping atom or ion. When $P_i > 0$, then the ion under consideration has a promoting effect on the catalytic rate and can cause NEMCA.

Thus in the present study P_i values up to 250 have been measured (e.g., Figs. 8a and 8b) which shows that indeed Na has a very pronounced promoting effect on the rate of CO oxidation on Pt when the rate is negative order in CO.

When $P_i < 0$, then the ion under consideration has a poisoning effect on the rate. In this case $(-P_i)$ equals the "toxicity" of the atom or ion, as defined by Barbier and co-workers (44). In the present study toxicity values up to 30 were measured (Figs. 3, 4b, 8b) for high Na coverages.

There are three major features of the observed steady-state NEMCA behaviour (Figs. 2–11) which must be explained:

I. The pronounced promoting effect of Na for $\theta_{Na} < 0.04$ when the rate is negative order in CO (Figs. 2, 3, 5, 6, 8, 9).

II. The pronounced poisoning effect of Na for $\theta_{Na} > 0.04$ and temperatures below 380°C (Figs. 2, 3, 5–10).

III. The observed pronounced dependence of activation energy on catalyst work function and temperature (Fig. 11).

These observations can be explained in a semiquantitative manner on the basis of our recent UHV study of oxygen, CO, and Na coadsorption on Pt (42), which demonstrated the formation of a CO–Na–Pt complex on Pt(111). The decomposition temperature of this complex (360°C) agrees well with the present results.

Observation (I) is clearly due to the promoting effect of Na on the kinetics (40) and thermodynamics of oxygen chemisorption on Pt. This is manifested in two ways:

(a) The promotional effect of Na appears only when the rate is negative order in CO, i.e., the surface has a very low coverage of oxygen (Figs. 2, 3, 4a, 5b, 8a, 8b, 9).

(b) The value of P^*_{CO} which maximizes the reaction rate (and implies, to a first approximation $\theta_{CO} \approx \theta_O$) is dramatically increased with increasing θ_{Na} (i.e., decreasing V_{WR} and $e\Phi$, Figs. 3, 6) which manifests a pronounced increase in the propensity of the surface to chemisorb O vs CO.

As shown in Fig. 2, in the promoting region the rate of CO oxidation increases exponentially with $e\Phi$ according to

$$\ln(r/r_0) = -\alpha\Delta e\Phi/k_bT, \qquad [10]$$

where $\alpha \approx 0.25$.

This observation can be easily rationalized within the framework of LHHW kinetics by taking into account the effect of decreasing $e\Phi$ on the binding strength of atomic oxygen and thus on the dissociative adsorption equilibrium constant of oxygen K_O. It is well known that LHHW kinetics can provide only an approximate and qualitative fit to the CO oxidation kinetics on Pt but nevertheless we have chosen to use them in order to rationalize in a simple semiquantitative manner observation I, i.e., Eq. [10] and, as shown below, observation III.

Assuming the reaction between chemisorbed CO and O to be rate limiting, one obtains the LHHW rate expression

$$r = k_R\theta_{CO}\theta_O = k_RK_{CO}K_OP_{CO}P_{O_2}^{1/2}/(1 + K_OP_{O_2}^{1/2} + K_{CO}P_{CO})^2, \qquad [11]$$

where k_R is the kinetic constant, and K_{CO} and K_O are the adsorption equilibrium constants for CO and oxygen, respectively.

The promoting effect of Na is observed when the $K_{CO}P_{CO}$ term dominates, in which case Eq. [11] reduces to

$$r = k_RK_OP_{O_2}^{1/2}/(K_{CO}P_{CO}). \qquad [12]$$

Although k_R, K_{CO}, and K_O are all expected to vary with changing Na coverage and $e\Phi$, one may, to a first approximation, assume that the effect on K_O is dominant so that

$$K_O = K_O^0 \exp(-\alpha\Delta e\Phi/k_bT). \qquad [13]$$

Combination of Eqs. [12] and [13] leads to the experimental Eq. [10]. The form of Eq. [13] is consistent with previous NEMCA studies which have shown linear variations in the heat of adsorption of oxygen on Pt with varying $e\Phi$ (2, 5).

The observed strengthening of the Pt=O bond with increasing θ_{Na} (decreasing $e\Phi$) is consistent with the general rules established in previous NEMCA studies on the effect of decreasing $e\Phi$ and thus enhanced back donation of electrons on the chemisorptive bond strength of electron acceptor adsorbates such as chemisorbed oxygen (2).

Observation II can be directly rationalized in terms of the formation of the CO–Na–Pt complex on the catalyst surface. As noted above, we have shown that such a CO–Na–Pt complex is indeed formed on Pt(111), decomposing at 360°C in UHV (42). A similar CO–K–Pt complex has been shown by Bertolini and co-workers (40) to form on Pt(100) and to decompose abruptly at 407°C (40). It is indeed remarkable that as shown on Figure 10 the temperature above which the CO–Na–Pt complex ceases to exist and thus poison the CO oxidation rate is between 385 and 410°C. Bertolini and co-workers showed that the CO–K–Pt surface complex forms on CO-covered Pt(100)

surfaces when the K coverage θ_K exceeds 0.3. Up to this K coverage there is a continuous strengthening in the CO chemisorptive bond with increasing θ_K as manifested by the gradual increase in the CO TDS temperature from 247 to 277°C (40).

The study of Bertolini *et al.* (40) also showed that K adsorption enhances oxygen chemisorption on Pt(100) which does not take place to any measurable extent on the K-free surface. The only difference from the present study is that high (>0.3)θ_K values were found necessary for the promoting role of K on O_2 chemisorption to become apparent, while in the present study low (~ 0.03) θ_{Na} values cause a pronounced enhancement in oxygen chemisorption (Figs. 4a, 8a, 8b).

Observation III, regarding the interesting and complex dependence of activation energy E on V_{WR} ($e\Phi$) and T can be rationalized within the framework of LHHW kinetics as follows:

The low activation energy value $E_1 = 2$ kcal/mol is obtained at high temperatures when the rate is positive order both in CO and oxygen. Under these conditions Eq. [11] reduces to

$$r = k_R K_{CO} K_O P_{CO} P_{O_2}^{1/2} \quad [14]$$

and consequently

$$E_1 = E_R - Q_{CO} - \tfrac{1}{2}Q_O, \quad [15]$$

where E_R is the true activation energy and Q_{CO} and $\frac{1}{2}Q_O$ are the heats of adsorption of CO and oxygen (kcal/mol).

In the region of CO inhibition the activation energy is $E_2 = 28$ kcal/mol, in good agreement with literature (45) and Eq. [12] is valid, therefore,

$$E_2 = E_R + Q_{CO} - \tfrac{1}{2}Q_O. \quad [16]$$

It follows then from Eqs. [15] and [16] that $Q_{CO} = 13$ kcal/mol. This value is low compared to the activation energy of desorption of CO at low coverages from clean Pt surfaces (typically 25–30 kcal/mol (45)) but in good agreement with apparent heats of adsorption at high coverages extracted by fitting atmospheric pressure high coverage kinetic data to LHHW kinetic expressions (30).

It also then follows from Equation [15] or [16] that $E_R - \frac{1}{2}Q_O = 15$ kcal/mol. The observed increase in E with decreasing V_{WR} in the region where oxygen chemisorption is enhanced ($0\ V > V_{WR} > -0.3\ V$) is physically due to the increase in oxygen coverage and can be described semiquantitatively by Eqs. [11] and [13] as shown by the dashed line in Fig. 11, where the following values were used for the parameters:

$$k_R = 3.7 \times 10^9 \text{ mol/cm}^2\text{ s} \quad [17a]$$

$$K_{CO} = 1.7 \times 10^{-5} \exp(13{,}000/RT) \text{ kPa}^{-1} \quad [17b]$$

$$K_O = 1.2 \times 10^{-13} \exp[[35{,}000 + \alpha(F/4.184)(-V_{WR})]/RT] \text{ kPa}^{-1/2}. \quad [17c]$$

Here $\alpha = 0.3$, $F = 96480$ C/mol, and V_{WR} varies between 0 and -0.3 V, i.e., in the region of exponential rate increase. The activation energy E can be easily computed on the basis of the following equation derived from Eq. [10]:

$$E = -R \cdot d(\ln r)/d(1/T)$$

$$= E_R - \frac{1}{2}Q_O - Q_{CO} + 2\frac{\frac{1}{2}K_O Q_O + K_{CO}Q_{CO}}{(1 + K_O + K_{CO})}. \quad [18]$$

For more positive potentials V_{WR} in Eq. [17c] is set equal to zero. The model computation of E (Fig. 11) for more negative potentials ($V_{WR} < -0.3$ V) is discussed below.

The very high E value $E_3 = 65$ kcal/mol for $V_{WR} < -0.3$ V, i.e., in the region of CO–Na–Pt complex formation where the rate decrease dramatically, can be explained semiquantitatively in the following terms: Given the properties of large oxocarbon species $[(CO_n)]^{2-}$ (46) it is plausible that even low Na coverages ($\theta_{Na} \sim 0.04$) lead to almost complete blocking of the Pt surface by the CO–Na–Pt complex. Under such conditions the activation energy for reaction will depend on the activation energy for decomposition Q_C of the surface complex. An estimate of 47 ± 5 kcal/mol for this quantity can be obtained from the Pt(100) data of Bertolini *et al.* (40). One can thus use the LHHW limiting rate expression (12), which is valid in the region of existence of the CO–Na–Pt complex (Fig. 9) to obtain the following expression for E_3, in analogy with Eq. [16]:

$$E_3 = E_R + Q_C - \tfrac{1}{2}Q_O. \quad [19]$$

Substituting $E_R - \frac{1}{2}Q_O = 15$ kcal/mol and $Q_C = 47$ kcal/mol, one obtains $E_3 = 62$ kcal/mol, in excellent agreement with the experimental value of 65 kcal/mol (Fig. 11). Although the quality of the agreement may be fortuitous, due to the inherent limitations of LHHW kinetics, it is clear that the high E value at very low V_{WR} values must indeed be due to the presence of the CO–Na–Pt complex.

In summary the present results show that the use of β''-Al_2O_3 as an active catalyst support to induce NEMCA leads to very pronounced and reversible alterations in the catalytic properties of Pt for CO oxidation. Sodium acts both as a promoter and as a poison for this catalytic reaction. Valuable information about the underlying rich chemistry can be obtained in the future by the use of surface spectroscopic techniques. Solid electrolytes, in

general, provide a unique way to *in situ* and precisely control the state of metal catalyst surfaces and to investigate the role of promoters in catalysis.

ACKNOWLEDGMENTS

We thank the CEC Science and Joule Programmes for financial support and our reviewers for helpful comments.

REFERENCES

1. Vayenas, C. G., Bebelis, S., and Ladas, S., *Nature (London)* **343** (6259), 625 (1990).
2. Vayenas, C. G., Bebelis, S., Yentekakis, I. V., and Lintz, H.-G., *in* "Catalysis Today," Vol. 11, No. 3, p. 303. Elsevier, Amsterdam, 1992.
3. Yentekakis, I. V., and Vayenas, C. G., *J. Catal.* **111,** 170 (1988).
4. Vayenas, C. G., Bebelis, S., and Neophytides, S., *J. Phys. Chem.* **92,** 5083 (1988).
5. Bebelis, S., and Vayenas, C. G., *J. Catal.* **118,** 125 (1989).
6. Neophytides, S., and Vayenas, C. G., *J. Catal.* **118,** 147 (1989).
7. Vayenas, C. G., Bebelis, S., Neophytides, S., and Yentekakis, I. V., *Appl. Phys. A* **49,** 95 (1989).
8. Vayenas, C. G., Bebelis, S., Yentekakis, I. V., Tsiakaras, P., and Karasali, H., *Platinum Met. Rev.* **34**(3), 122 (1990).
9. Vayenas, C. G., and Neophytides, S., *J. Catal.* **127,** 645 (1991).
10. Vayenas, C. G., Bebelis, S., and Despotopoulou, M., *J. Catal.* **128,** 415 (1991).
11. Ladas, S., Bebelis, S., and Vayenas, C. G., *Surf. Sci.* **251/252,** 1062 (1991).
12. Vayenas, C. G., Bebelis, S., and Kyriazis, C., CHEMTECH **21,** 500 (1991).
13. Vayenas, C. G., Bebelis, S., Yentekakis, I. V., and Neophytides, S., *Solid State Ionics* **53–56,** 97 (1992).
14. Bebelis, S., and Vayenas, C. G., *J. Catal.* **138,** 570 (1992).
15. Bebelis, S., and Vayenas, C. G., *J. Catal.* **138,** 588 (1992).
16. Tsiakaras, P., and Vayenas, C. G., *J. Catal.* **140,** 53 (1993).
17. Yentekakis, I. V., and Bebelis, S., *J. Catal.* **137,** 278 (1992).
18. Cavalca, C. A., Larsen, G., Vayenas, C. G., and Haller, G. L., *J. Phys. Chem.* **97,** 6115 (1993).
19. Alqahtany, H., Chiang, P., Eng, D., and Stoukides, M., *Catal. Lett.* **13,** 289 (1992).
20. Politova, T. I., Sobyanin, V. A., and Belyaev, V. D., *React. Kinet. Catal. Lett.* **41,** 321 (1990).
21. Mar'ina, O. A., and Sobyanin, V. A., *Catal. Lett.* **13,** 61 (1992).
22. Pritchard, J., *Nature (London)* **343,** 592 (1990).
23. Arakawa, T., Saito, A., and Shiokawa, J., *Chem. Phys. Lett.* **94,** 250 (1983); *Appl. Surf. Sci.* **16,** 365 (1983).
24. Vöhrer, U., Ph.D. Thesis, Universität Tübingen, 1992.
25. Ladas, S., Kennou, S., Bebelis, S., and Vayenas, C. G., *J. Phys. Chem.* **97,** 8845 (1993).
26. Razon, L. F., and Schmitz, R. A., *Catal. Rev.-Sci. Eng.* **28,** 89 (1986).
27. Engel, T., and Ertl, G., *in* "The Chemical Physics of Solid Surfaces and Heterogeneous Catalysis" (D. A. King and D. P. Woodruff, Eds.), Vol. 4. Elsevier, Amsterdam, 1982.
28. Coulston, G., and Haller, G. L., *in* "Surface Science of Catalysis: In situ probes and reaction Kinetics" (D. J. Dwyer and F. M. Hoffmann, Eds.), ACS Symposium Series, Vol. 482, p. 58. Am. Chem. Soc., Washington, DC, 1992.
29. Akhter, S., and White, J. M., *Surf. Sci.* **171,** 527 (1986).
30. Yentekakis, I. V., Neophytides, S., and Vayenas, C. G., *J. Catal.* **111,** 152 (1988).
31. Hegedus, L. L., and Gumbleton, J., CHEMTECH **642** (1980).
32. Matsushima, T., *J. Catal.* **55,** 337 (1978); *Surf. Sci.* **79,** 63 (1979).
33. Hölzl, J., and Schulte, F. K., *in* "Solid Surface Physics" (J. Hölzl *et al.*, Eds.), p. 1. Springer-Verlag, Berlin, 1979.
34. Schröder, W., and Hölz, J., *Solid State Commun.* **24,** 777 (1977).
35. Bonzel, H. P., *Surf. Sci. Rep.* **8,** 43 (1987).
36. Heskett, D., *Surf. Sci.* **199,** 67 (1988).
37. Aruga, T., and Murata, Y., *Prog. Surf. Sci.* **31,** 61 (1989).
38. Uram,K.J., Ng, L., and Yates, J. T., Jr., *Surf. Sci.* **177,** 253 (1986).
39. Haruta, M., Tsubota, S., Kobayashi, T., Ueda, A., Sakurai, H., and Ando, M., *in* "New Frontiers in Catalysis" (L. Guczi *et al.*, Eds.), p. 2657. Elsevier, Amsterdam, 1993.
40. Bertolini, J. C., Delichere, P., and Massardier, J., *Surf. Sci.* **160,** 531 (1985).
41. Goddard, P. J., and Lambert, R.M., *Surf. Sci.* **107,** 519 (1981).
42. Harkness, I. R., Yentekakis, I. V., Vayenas, C. G., and Lambert, R. M., in preparation.
43. Hardacre, C., Ormerod, R. M., and Lambert, R. M., *Chem. Phys. Lett.* **206,** 171 (1993).
44. Lamy-Pitara, E., Bencharif, L., and Barbier, J., *Appl. Catal.* **18,** 117 (1985).
45. Berlowitz, P.J., Peden, C. H. F., and Goodman, D. W., *J. Phys. Chem.* **92,** 5213 (1988).
46. West, R., and Niu, J., *in* "The Chemistry of the Carbonyl Group" (J. Zabicky, Ed.), Vol. 2. Wiley–Interscience, New York, 1970.